# Field measurements from contrasting reefs show spurs and grooves can dissipate more wave energy than the reef crest

**S. Duce[1,2], A. Vila-Concejo[2], R. J. McCarroll[2,3], B. Yiu[4], L. A. Perris[2], and J. M. Webster[2]**

[1]TROPwater, College of Science and Engineering, James Cook University, Bebegu Yumba Campus, Townsville, Queensland, 4811, Australia

[2]Geocoastal Research Group, School of Geosciences, University of Sydney, Sydney, New South Wales, 2006, Australia.

[3]Department Environment, Land, Water and Planning, East Melbourne, Victoria, Australia

[4]Field Sampling & Testing, Sydney Water, 51 Hermitage Road, West Ryde, NSW, 2114, Australia

Corresponding author: Stephanie Duce (stephanie.duce@jcu.edu.au )

**Key Points:**

- Field measurements show extremely high wave energy dissipation rates (up to 0.1 kW/m$^2$) across the SAG zone due to bottom friction alone.
- SAGs were more effective at dissipating wave energy than the reef crest across differing reef morphologies and hydrodynamic regimes.
- Greater dissipation at sites with high coral cover and mesotidal range suggest live coral and tidal currents contribute to dissipation.

## Abstract

Coral reefs are widely recognized as effective dissipaters of wave energy. Spurs and grooves (SAG) are common features of fore reefs worldwide and are thought to be particularly efficient at dissipating wave energy. However, very few studies have collected in-situ hydrodynamic data to verify this and understand SAG interactions with hydrodynamic forces. We present in-situ wave data from contrasting SAG sites at Moorea, French Polynesia and One Tree Reef in the southern Great Barrier Reef, Australia. We measured extremely high rates of wave energy dissipation (up to 0.1 $kW/m^2$) across the SAG zone due to bottom friction alone. Interestingly, SAGs dissipated wave energy at higher rates than the reef crest under the modal conditions measured. Rates of dissipation were the greatest at sites with high live coral cover in mesotidal environments (i.e., One Tree Reef), suggesting the structural complexity of live corals increases bed friction and that tidal currents may contribute to dissipation. Unexpectedly, rates of dissipation were higher across the groove (mean $\in$=0.04 $kW/m^2$) than the adjacent spur (mean $\in$=0.01 $kW/m^2$). Correlations between measured dissipation, wave height and depth allowed us to develop a conceptual model showing that SAGs dissipate more energy under high wave conditions at low tides, while the reef crest dissipates more energy at high tides under small wave conditions. Further study is required to better understand and model the hydrodynamics of SAG zones and the important role they play in reef dynamics and coastal protection.



## Plain Language Summary

Coral reefs play an essential role in reducing the impact of waves on adjacent coastal areas and infrastructure. However, due to the difficulty of working in high energy wave environments, little is known about how different reef zones dissipate wave energy. To address this research gap, we used pressure sensors to measure the height and power of waves across different coral reef zones at One Tree Reef in the Great Barrier Reef, Australia, and Moorea in French Polynesia. We examined how waves dissipate their energy as they move across the reef from the fore reef, a deeper zone characterised by finger-like coral structures called spurs and grooves, to the reef crest, a shallower area where waves often break, and which is assumed to be responsible for most wave energy dissipation. Surprisingly, we found that the fore reef spur and groove zone was often more effective in dissipating wave energy than the reef crest. Tidal stage and wave height were important in determining how much the

waves interact with the seafloor and loose energy due to friction. Our study also found initial evidence that the amount of live coral cover is important, with higher dissipation found in areas with higher live coral cover. Further field studies measuring wave dissipation across reef zones will help us better understand and model this system and its importance in coastal protection.

## 1. Introduction

Waves are the main hydrodynamic force acting on coral reefs and are a crucial driving factor in the formation, growth and persistence of coral reefs across all spatial and temporal scales (Harris et al., 2015; Storlazzi et al., 2005). Reef hydrodynamics control the transport and deposition of spawn, larvae and recruits, the provision of nutrients, removal of wastes and the production and transport of biogenic sediments to form the reef and associated features such as reef islands (Masselink et al., 2020). Coral reefs have long been recognized as providing effective wave energy dissipation and protecting coastlines (e.g. Munk & Sargent, 1948). The value of reefs as natural breakwater systems has become particularly important with growing threats from rising sea levels and increased storm activity (e.g. Beck et al., 2018; Ferrario et al., 2014; Foley et al., 2014; Gallop et al., 2014; Van Zanten et al., 2014; Vila-Concejo et al., 2017; Woodhead et al., 2019).

Numerical modelling of wave dissipation across coral reefs has become a relatively common tool to inform coastal management and predict the likely effects of sea level rise (Baldock et al., 2019; Baldock et al., 2020; Bramante et al., 2020; Harris et al., 2018). Accurate and high-resolution field data are required to calibrate and validate numerical models and optimize their utility (e.g. Horstman et al., 2014; Storlazzi et al., 2011). However, the remote location of many coral reefs makes access difficult, and it is challenging to deploy instruments particularly in the high-energy fore reef zone. Nevertheless, field observations in fore reef environments are necessary to examine dissipation under complex natural conditions and to understand sediment production and transport in biogenic coral reef systems.

The majority of existing studies detailing wave dissipation by coral reefs measure dissipation across reef flats (e.g. Brander et al., 2004; Hardy & Young, 1996; Harris & Vila-Concejo, 2013; Harris et al., 2015; Huang et al., 2012; Kench & Brander, 2006) and around reef islands (e.g. Beetham & Kench, 2014; Kench et al., 2009; Mandlier, 2013; Samosorn &

Woodroffe, 2008). Given the logistical complexity of instrument deployments on reefs, some studies have measured wave dissipation across the reef crest based on a single instrument on the fore reef and another on the reef flat behind the reef crest (e.g. Lowe, 2005; Lugo-Fernández et al., 1998a; Lugo-Fernández et al., 1998b; Pomeroy et al., 2012; Cheriton et al., 2016). These studies provide robust evidence of coral reefs' ability to dissipate wave energy but do not provide spatial resolution to differentiate wave dissipation occurring on the fore reef from that of the reef crest and reef flat. Notable exceptions are Monismith et al. (2015), Monismith et al. (2013), Péquignet et al. (2011) and Storlazzi et al. (2004), where wave measurements included at least two fore reef locations. On the fore reef of Palmyra Atoll, Monismith et al. (2015) calculated the highest friction factor (1.8) measured at any reef, with approximately 20% wave energy dissipation over 56 m (i.e., 35.7% over 100 m) and suggested that healthy coral cover facilitated efficient wave dissipation.

Spurs and grooves (SAG) are a common geomorphic feature of many fore reefs worldwide and their origin and formation mechanisms have been the subject of some debate (Gischler, 2010). They are characterized by parallel ridges of carbonate material (spurs), separated by channels (grooves) which are usually aligned perpendicular to the reef front. The features show considerable variations in morphology which are thought to be predominantly driven by the prevailing hydrodynamic energy (Duce et al., 2020; Duce et al., 2016; Roberts, 1974; Storlazzi et al., 2003). However, very few studies have collected in-situ hydrodynamic data to verify this, let alone attempt to understand the mechanics and spatial variability of wave energy dissipation by the SAG.

To date wave hydrodynamics across SAGs have only been directly measured at three reefs worldwide; Grand Cayman Island in the Caribbean (Roberts et al., 1975), Molokai, Hawaii (Storlazzi et al., 2004) and Ipan, Guam (Péquignet et al., 2011) in the central Pacific. At Grand Cayman, Roberts et al. (1975) found that bottom friction at the fore reef SAGs modified deep water waves and currents reducing wave heights by ~20% (i.e., 0.5% per 10 m) and current speeds by ~60-70% over the ~400 m between the outer instrument (21 m depth) and inner instrument (8 m depth). Storlazzi et al. (2004) measured less than 0.1% dissipation in wave power per 10 m for small waves ($Hs$ <0.4 m) across the SAG zone at Molokai, Hawaii. Péquignet et al. (2011) measured a 17% decline in wave energy flux during a tropical cyclone over 55 m (i.e., 3.1% per 10 m) between sensors at 7.9 and 5.7 m depth on the fore reef SAGs at Ipan fringing reef in Guam and found that the majority of energy was dissipated by wave breaking in the surf zone.

In this paper, we quantify the wave energy dissipation across different types of SAG in two contrasting coral reef types and determine the mechanisms by which most dissipation occurs at each site (i.e., wave breaking at the reef crest versus bottom friction across the fore reef). Further, we assess the influence of other variables including offshore wave height, water depth, spur and groove morphology, tidal currents and coral cover on energy dissipation. This paper also presents comprehensive wave datasets, including measurements at the inner and outer limits of the SAG zone at five sites located on two contrasting reefs under different tidal and wave energy regimes. These sites are Moorea in French Polynesia and One Tree Reef in the southern Great Barrier Reef (GBR).

## 2. Study Sites

We undertook 10 field experiments, five at One Tree Reef in the southern GBR, Australia and five at Moorea, French Polynesia. The field experiments included areas from each reef with different degrees of wave exposure (Figures 1 and 2) with wave measurements undertaken across the SAG zone of the fore reef. Each site is described in detail in Supplementary Text S1-S5.

### 2.1 Moorea

Moorea (17°30' S, 149°50' W) is a high volcanic island in French Polynesia, in the central tropical South Pacific Ocean (Figure 1). The island has a perimeter of 60 km and is surrounded by a barrier reef between 0.5 to 1 km from shore protecting an inshore lagoon (Leichter et al., 2012). Several passes around the reef connect the inshore lagoons with the open ocean (Figure 1b). Between 1 and 2 km offshore of the reef, water depths drop to > 500 m (Leichter et al., 2013). Moorea is micro-tidal with a spring tidal range of 0.2 m (Hench et al., 2008). It is exposed to seasonal oceanic swells with significant wave heights between 1 and 2 m, however significant wave heights between 5 to 8 m, associated with storms and remotely generated swell, are not uncommon (Leichter et al., 2013). The dominant swell direction is from the southwest. From approximately October to April, the northern shore of Moorea receives northerly swells driven by storms across the Northern Pacific (Hench et al., 2008). Waves are the dominant driver of currents over the reef crest as tides and wind-driven flows are relatively weak (Hench et al., 2008; Monismith et al., 2013).

Since quantitative scientific studies began in the 1970s, Moorea reef has experienced a number of stressors in the form of recurrent bleaching events (Adjeroud et al., 2009), two major outbreaks of Crown-of-Thorns sea stars (Trapon et al., 2011) and cyclones, particularly

Cyclone Oli in 2010 (Etienne, 2012). These events caused coral cover on the fore reef to decline from > 40% in 2005 to < 5% in 2010 (Kayal et al., 2012). By 2013 Scleractinian coral cover at Moorea fore reef (10 m depth) had recovered to approximately 20% and was composed almost entirely of juveniles (Edmunds & Leichter, 2016). SAGs are visible in satellite imagery around the entire fore reef of the barrier system.

## 2.2 One Tree Reef

One Tree Reef (OTR, 23°30′ S, 152°05′ E) is a lagoonal (mature) reef in the Capricorn-Bunker Group of reefs in the southern GBR (Hopley et al., 2007). The reef lies within a "Scientific Zone" of the GBR Marine Park, 80 km seaward of mainland Australia and hence has minimal anthropogenic influences. It is located only 20 km west of the edge of the continental shelf and is therefore exposed to the southeast trade winds and modal swell energy for most of the year (Frith and Mason, 1986). The average annual significant wave height is approximately 1.15 m from a predominantly east southeasterly direction driven by trade winds (Hopley et al., 2007) and occasional cyclones also occur (e.g. Woolsey et al., 2012). The reef is mesotidal and has semidiurnal tides with a mean spring tidal range of 3 m (Vila-Concejo et al., 2014). The reef crest is mostly unbroken with no clear passes, and the lagoon is isolated from swell and tides during approximately five hours of each tidal cycle (Frith & Mason, 1986). There are high levels of live coral cover, particularly on the fore reef, and a diverse range of calcifiers are present (Hamylton et al., 2013). SAGs are present around the entire fore reef with four distinct classes associated with the different levels of wave energy and antecedent topography (Duce et al., 2016). Duce et al. (2020) demonstrated that the formation and evolution of SAGs at OTR could include growth offshore or onshore depending primarily on wave exposure. The presence of a rubble cay on the southwest corner of the reef flat and several active rubble spits along the reef flats demonstrate sediment transport from the fore reef (Bryson et al., 2016; Shannon et al., 2013).

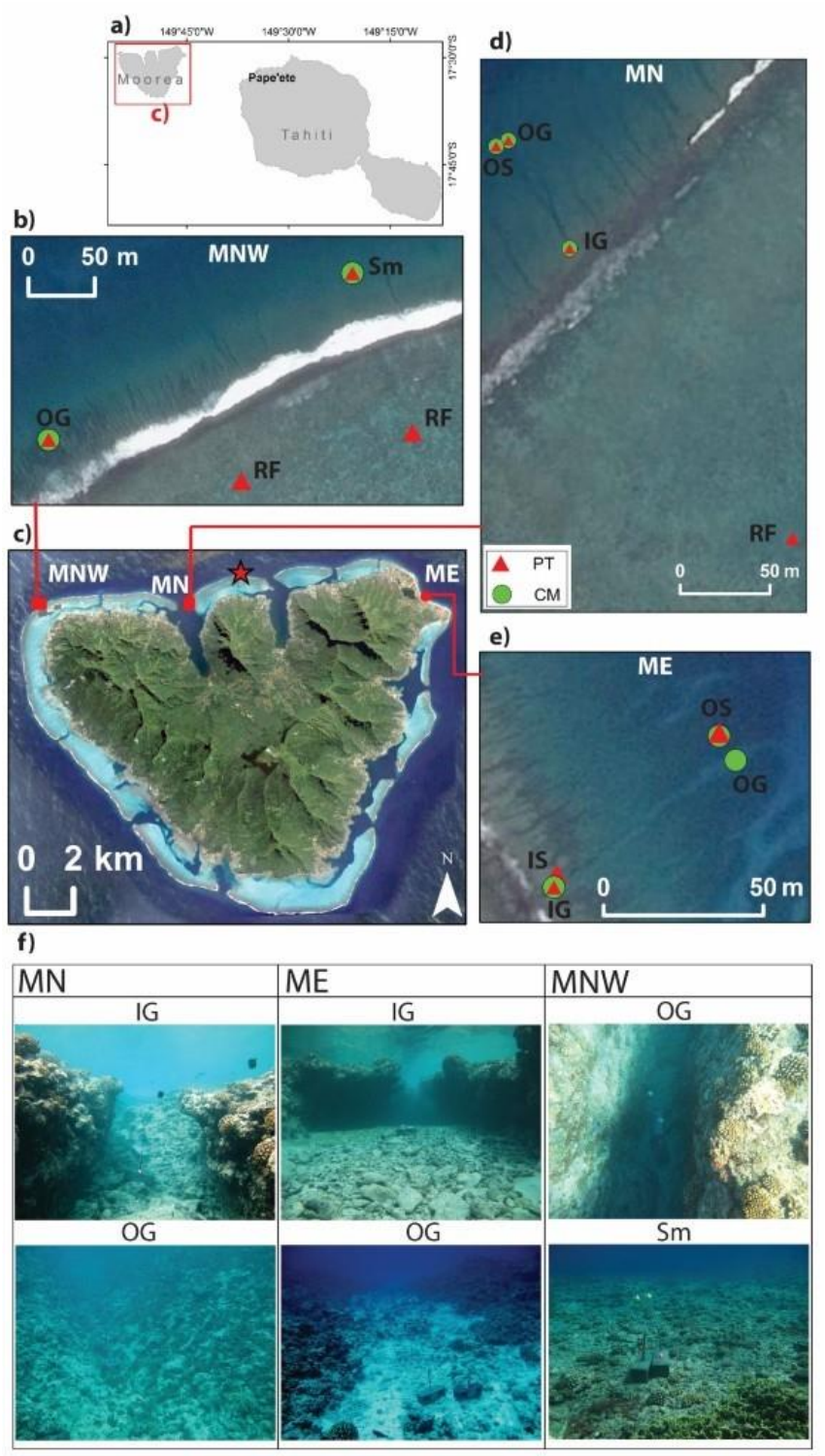


**Figure 1** The location of Moorea adjacent to Tahiti in the South Pacific Ocean (a). Panel (c) shows an overview of the island where the star represents the location of the FOR01 wave mooring. Imagery of the study sites Moorea Northwest (MNW) (b); Moorea North (MN) (d) and Moorea East (ME) (e) are presented. The position of pressure sensors (PS - triangles) and current meters (CM – circles, Note: current meter data is not presented in this paper) are shown and labelled IG (inner groove), OG (outer groove), OS (outer spur), IS (inner spur), SFR (smooth fore reef) and RF (reef flat). Photographs of the deployment sites are shown in (f).

192

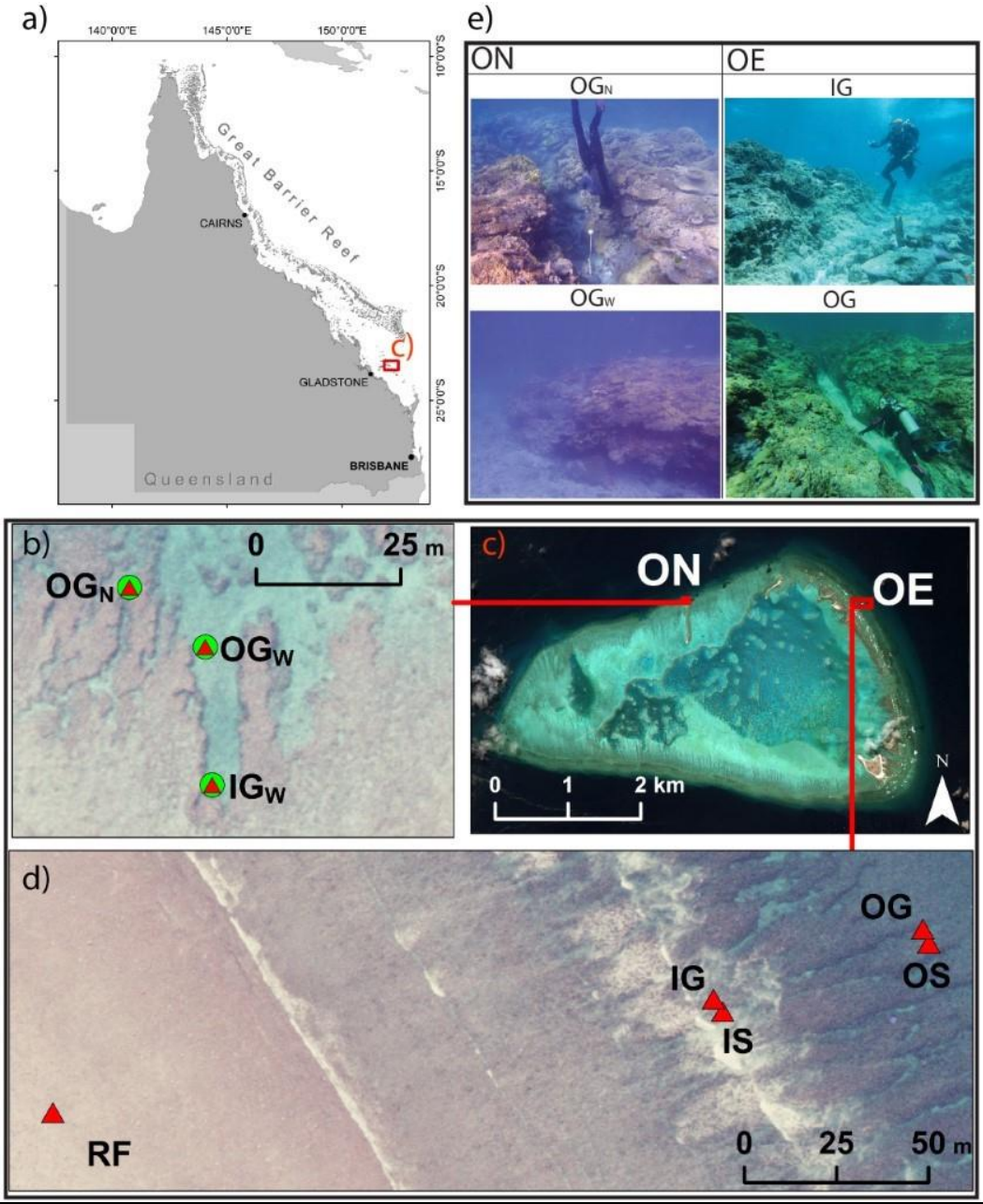


**Figure 2** Overview of the location of One Tree Reef in the southern Great Barrier Reef (a) and the position of study sites around the reef (c). The position of pressure sensors (PS - triangles) and current meters (CM – circles. Note: current meter data is not presented in this paper) at One Tree north (ON) (b) and One Tree east (OE) (d) are shown and labelled IG (inner groove), OG (outer groove), OS (outer spur), IS (inner spur) and RF (reef flat). At ON (b) subscript $_N$ denotes narrow groove and $_W$ denotes wide groove. Photographs of the deployment sites are presented in (e).

## 3. Methods

### 3.1 Offshore wave data

Offshore wave data during our deployments at Moorea were obtained from the Moorea Coral Reef Long-Term Ecological Research (MCR LTER) mooring FOR01 on the northern fore reef (17.475°S, 149.837°E, Figure 1c) at a depth of approximately 10 m (Washburn,

2015) and from the WaveWatch III (WW3) global hindcast wave model (Tolman, 2009). Wind data were obtained from Gump Station (Washburn & Brooks, 2016). Offshore wave data at One Tree Reef were obtained from a Nortek Acoustic Waves and Currents Sensor (AWAC) deployed at the One Tree East Mooring (23° 28.999' S, 152° 10.356' E) at a depth of 15 m on the continental shelf 8 km east of One Tree Reef. Wind data were obtained from the Australian Institute of Marine Science Integrated Marine Observing Station (AIMS IMOS) weather station in the One Tree lagoon.

### 3.2 Data collection

The SAG zone, particularly the shallow area adjoining the reef crest, is extremely dynamic and difficult to deploy instruments in, which explains the paucity of data collected in this area to date. We deployed Aquistar INW PT2X pressure sensors at all sites, sampling continuously at 4 Hz to measure wave characteristics. The length of the deployments was typically short (<24 h) due to limited data storage in the instruments. The instruments were cable tied to purpose-built concrete blocks with protruding metal rods that were placed by SCUBA divers using lift bags. As shown by Duce et al. (2016) and Duce et al. (2020), the same reef can support different SAG types thus deployments were conducted at multiple sites on each reef to capture differing wave exposure regimes. Deployment locations included three sites on the fore reef at Moorea – Moorea North West (MNW), Moorea North (MN) and Moorea East (ME) (Figure 1); and two sites at One Tree Reef – One Tree East (OE) and One Tree North (ON) (Figure 2). Detailed descriptions of each of these sites and the instrument deployment configuration are available in Table 1 and the supplementary materials (Supp. 1).

**Table 1** Overview of the deployments at Moorea and One Tree reefs including the geomorphic characteristics of the site and the dates of each deployment. For further information on each site refer to S1-S5. (The following acronyms are used in this table: MN: Moorea North; ME: Moorea East; MNW: Moorea North West; OE: One Tree East; ON: One Tree North; IG: Inner Groove; OG: Outer Groove; RF: Reef Flat; IS: Inner Spur; OS: Outer Spur; SFR: Smooth fore reef; W: wide; N: narrow)

| Location | Deployment | Site | Depth (m) | Approx. width (m) | Approx. spur wall height (m) | Dist. seaward of crest (m) | Dates | Site Descriptions/Comparisons |
|---|---|---|---|---|---|---|---|---|
| Moorea | Moorea North 1 | MN1-IG | 3.3 | 2 | 0.6 | 20 | Aug to 9 Aug 2014 | - Moderately exposed compared to other Moorea sites<br>- SAG zone width ~100 m and gradient ~5° to a depth of ~12 m<br>- Reef crest and flat submerged throughout the tidal cycle<br>- Coral cover ~10-20%<br>- Bottom of grooves are bare or have large, rounded rubble grading to patches of coarse sand with depth |
| | | MN1-OG | 9.1 | 5 | 4 | 90 | | |
| | | MN1-RF | 1.9 | - | - | - | | |
| | Moorea North 2 | MN2-IG | 3.3 | 2 | 0.6 | 20 | 11 Aug 2014 | |
| | | MN2-OG | 8.9 | 5 | 4 | 90 | | |
| | | MN2-OS | 4.7 | 20 | 4 | 90 | | |
| | | MN2-RF | 1.9 | - | - | - | | |
| | Moorea East 1 | ME1-IG | 3.8 | 4 | 1.5 | 15 | 19 Aug to 20 Aug 2014 | - Least exposed of Moorea sites<br>- SaG zone width ~100 m and gradient ~8˚ to a depth of ~16 m<br>- Reef crest and flat submerged throughout the tidal cycle<br>- Coral cover ~25%<br>- Bottom of grooves have large, rounded rubble grading to small angular rubble and sand with depth |
| | | ME1-IS | 2.7 | 6 | 1.5 | 18 | | |
| | | ME1-OS | 7.0 | 20 | 3 | 85 | | |
| | Moorea East 2 | ME2-IG | 3.8 | 4 | 1.5 | 15 | 21 Aug 2014 | |
| | | ME2-IS | 2.7 | 6 | 1.5 | 18 | | |
| | | ME2-OS | 7.7 | 20 | 3 | 85 | | |
| | Moorea North West | MNW-OG | 5.8 | 1.5 | 2.5 | 54 | 15 Aug to 16 Aug 2014 | - Most exposed of Moorea sites (unable to deploy instruments at inner groove or on spur due to high energy waves breaking)<br>- SaG zone width ~70 m and gradient ~6˚ to a depth of ~8 m<br>- Reef crest and flat submerged throughout the tidal cycle<br>- Coral cover ~40%.<br>- Bottom of grooves bare, with occasional large |
| | | MNW-$RF_{SAG}$ | 1.1 | - | - | - | | |
| | | MNW-SFR | 3.6 | - | - | 56 | | |
| | | MNW-$RF_{SFR}$ | 1.4 | - | - | - | | |

| | | | | | | | | |
|---|---|---|---|---|---|---|---|---|
| | | | | | | | | rounded coral boulders<br>- A 150 m long area of smooth fore reef (SFR) between SAGS |
| One Tree | One Tree East | OE-IG | 2.8 | 1.5 | 1 | 28 | 11 Oct<br>to<br>13 Oct 2013 | - Most exposed of One Tree sites<br>- SAG zone width ~120 m with gradient of ~2° to a depth of 6 m<br>- classified as "exposed to wave energy" (EWE) by Duce et al. (2016)<br>- Reef crest and flat exposed and therefore disconnected from SAGs over low tides<br>- Coral cover ~75%<br>- Bottom of grooves have large, smoothed rubble clasts transitioning to coarse rippled sand with depth |
| | | OE-OG | 5.4 | 2 | 2.5 | 88 | | |
| | | OE-IS | 1.9 | 7 | 1 | 28 | | |
| | | OE-OS | 2.5 | 10 | 2.5 | 88 | | |
| | | OE-RF | 0.6 | - | - | - | | |
| | One Tree North 1 | ON1-$IG_W$ | 2.9 | 5.0 | 1.5 | 10 | 1 Dec 2014 | - Least exposed of One Tree sites<br>- SAG zone with ~200 m with gradient of ~4° to a depth of ~10 m<br>- Outer groove narrow (OGN) classified as "short and protected" (SaP); neighbouring wide groove (IGW and OGW) classified as "long and protected" (LaP) by Duce et al. (2016)<br>- Reef crest and flat exposed and therefore disconnected from SAGs over low tides<br>-Coral cover ~85%<br>- Bottom of the narrow groove and the outer end of the wider groove have poorly sorted, angular coral rubble and little sediment. Inner end of the wide groove has sand with some angular rubble and occasional live corals. |
| | | ON1-$OG_W$ | 2.9 | 8.5 | 2.0 | 34 | | |
| | | ON1-$OG_N$ | 2.1 | 1.5 | 1.0 | 29 | | |
| | One Tree North 2 | ON2-$IG_W$ | 3.0 | 5.0 | 1.5 | 10 | 2 Dec<br>to<br>3 Dec 2014 | |
| | | ON2-$OG_W$ | 3.2 | 8.5 | 2.0 | 34 | | |
| | | ON2-$OG_N$ | 2.4 | 1.5 | 1.0 | 29 | | |
| | One Tree North 3 | ON3-$IG_W$ | 3.5 | 5.0 | 1.5 | 10 | 5 Jan 2015 | |
| | | ON3-$OG_W$ | 3.6 | 8.5 | 2.0 | 34 | | |
| | | ON3-$OG_N$ | 2.8 | 1.5 | 1.0 | 29 | | |
| | One Tree North 4 | ON4-$IG_W$ | 3.5 | 5.0 | 1.5 | 10 | 7 Jan<br>to<br>8 Jan 2015 | |
| | | ON4-$OG_w$ | 3.7 | 8.5 | 2.0 | 34 | | |

### 3.3 Data Analysis

Spectral analysis of pressure sensor data was conducted using a Fourier transform algorithm for 15-minute intervals with 50% overlap. A Hanning window was applied with linear detrending. A dynamic pressure adjustment, based on Lee and Wang (1984), was performed to account for pressure attenuation with depth and convert the subsurface pressure record to surface waves. Linear wave theory has been shown to perform well in steep, complex reef environments (Monismith et al., 2013). Thus, standard shallow water linear wave theory was used to calculate the significant wave height ($H_s$) peak wave period ($T_p$) and wave power ($P$).

$$P = 1/8\rho p g H_s^2 Hs^2 \sqrt{gh} \quad (1)$$

where, $\rho$ is the density of sea water (1027 kg/m$^3$), $g$ is the gravitational acceleration (9.81 m/s$^2$) and $h$ is water depth (m). Given the considerable number of deployments (10) and instrument records (33) it is not practical to present the wave spectra or time series of wave parameters for each instrument here. Instead, and to allow for comparison, we made box plots in SPSS showing the median, first and third quartile of values recorded at each instrument during each deployment.

We calculated energy dissipation rate per meter and percent of total energy dissipated between outer and inner groove instruments and between inner groove and reef flat instruments. Rates of wave energy dissipation ($\in$) in kilowatts per square meter (kW/m$^2$) were calculated using the following formula (based on Monismith et al. (2015)):

$$\in = \frac{\Delta P}{\Delta x} \quad (2)$$

where, $\Delta P$ is the change in wave power (kW/m) between the outer and inner instruments and $\Delta x$ is the across reef distance in meters, between the two instruments. Following the findings of Monismith et al. (2013), it was assumed that the direction of the incident wave field was perpendicular to groove orientation. The effects of wave reflection were reported to be minimal at a similar fore reef environment (Monismith et al., 2015) and therefore were not considered. This method assumes wave energy is dissipated at a uniform rate between the two instruments at which it is measured. While this is a reasonable assumption for unbroken

waves on the fore reef (OG-IG) when dissipation is due to bottom friction alone, it does not hold when wave breaking occurs between two instruments. This is a limitation which must be considered particularly when interpreting the dissipation rates calculated between the fore reef and the reef flat (IG-RF).

To determine whether wave breaking would have been a factor in dissipating wave energy we defined the wave breaking parameter such that:

$$\gamma = H_{max}/h \quad (3)$$

where, $H_{max}$ is double $H_s$ and $h$ is water depth. Published wave breaking parameters measured on coral fore reef environments vary from 0.83 (Rogers et al., 2016) to 0.98 (Monismith et al., 2013) up to 1.1 (Vetter et al., 2010). We chose a conservative estimation (0.6) as we were interested in assessing the contribution of bottom friction to wave dissipation in the absence of breaking, thus we needed to be sure that waves would not have been breaking at our fore reef instruments.

## 4. Results

### 4.1 Offshore wave and wind conditions

#### 4.1.1 Moorea

During the study period in August 2014 the offshore wave climate at Moorea, obtained from WW3, was dominated by south, southwesterly swell with mean significant wave height of 2.0 m (Supp. Figure 1). The waves recorded at FOR01 on the northern reef had a mean $H_s$ of 0.6 m, a maximum $H_s$ of 1.2 m and a $T_p$ of 8 seconds. Waves approached from a northerly direction (Supp. Figure 1 c) suggesting that the offshore waves obtained from the WW3 model had refracted around the northern side of the island. Local winds at Moorea have previously been reported to have minimal effects on hydrodynamic circulation and thus were not examined in this study (Hench et al., 2008).

#### 4.1.2 One Tree

The mean offshore significant wave height during the One Tree East deployment (11-13 Oct 2013) was 0.78 m with a maximum $H_s$ of 1.1 m and $T_p$ of 5 s (Supp. Figure 2). During this deployment the offshore wave direction was north-northeasterly, and winds were northerly. During the One Tree North deployments (Nov 2014 to Jan 2015) the mean offshore $H_s$ was

1.5 m with a maximum $H_s$ of 3.4 m and a $T_p$ of 7 seconds. Waves were predominately from the east (Figure 4c). The average maximum wind speed during One Tree North deployments was 29 km/h from an easterly direction (Supp. Figure 3d). During One Tree North deployment 4 (7-8 Jan 2015) there was a relatively high energy event with maximum offshore $H_s$ reaching 3 m and a maximum wind speed (i.e., the highest speed recorded each 30 min period) of 54 km/h from the east (Supp. Figure 3e).

### 4.2 Wave conditions in the SAG zone

Measured mean $H_s$ were relatively small (<1 m) during all deployments with wave conditions during each deployment varying across the SAG zone (Figure 3). Spectral analysis revealed the dominant energy component to be the incident frequency band (3-25 s) for all deployments. Time series of wave conditions for all deployments are provided in the Supplementary material (Supp. Figures 4-13). The conservative wave breaking parameter was exceeded only at the outer and inner spurs, and the inner groove at One Tree East during part of the first low tide. No other instruments showed wave breaking though it is assumed that breaking would have occurred at the reef crest between the inner SAG instruments and the reef flat instruments.

$P$ was greatest at the deepest and furthest seaward instruments (usually outer groove instruments) for all deployments (Figure 3). The largest waves (mean $H_s$ = 0.86 m, $P$ = 7kW/m) were recorded at the outer groove at Moorea North West (Figure 3 e, o), followed by both spurs and grooves at One Tree East (Figure 3f, p) and Moorea East 2 (Figure 3d, n). The smallest and least powerful waves for all deployments were recorded at the reef flat instruments. Regardless of wave height offshore, under modal conditions such as those recorded, virtually all power and height was dissipated by the time the waves reached the reef flat.

When comparing data from adjacent inner spur and inner groove we found that at Moorea East mean $H_s$ and $P$ for both deployments were higher at the spur (up to 2.61 kW/m) than the groove (up to 2.15 kW/m, Figure 3m, n), which could be related to increased shoaling over the spurs. Conversely, at One Tree East the inner groove had slightly higher $H_s$ and $P$ (2 kW/m) than the adjacent inner spur (1.6 kW/m) (Figure 3p). The instruments were approximately one meter shallower than at Moorea East (OE inner spur depth 1.9 m and groove 2.9 m vs 2.7 m and 3.8 m at ME) (Table 1), suggesting that as waves propagate

further across the SAG zone, bottom friction influences waves at the spur more than the groove. At sites where we conducted more than one deployment (i.e., MN, ME and ON) despite changes in the magnitude of $H_s$ and $P$ the pattern of wave characteristics within the zone was consistent between deployments (e.g., at ME power was highest at the outer spur, followed by the inner spur then the inner groove).

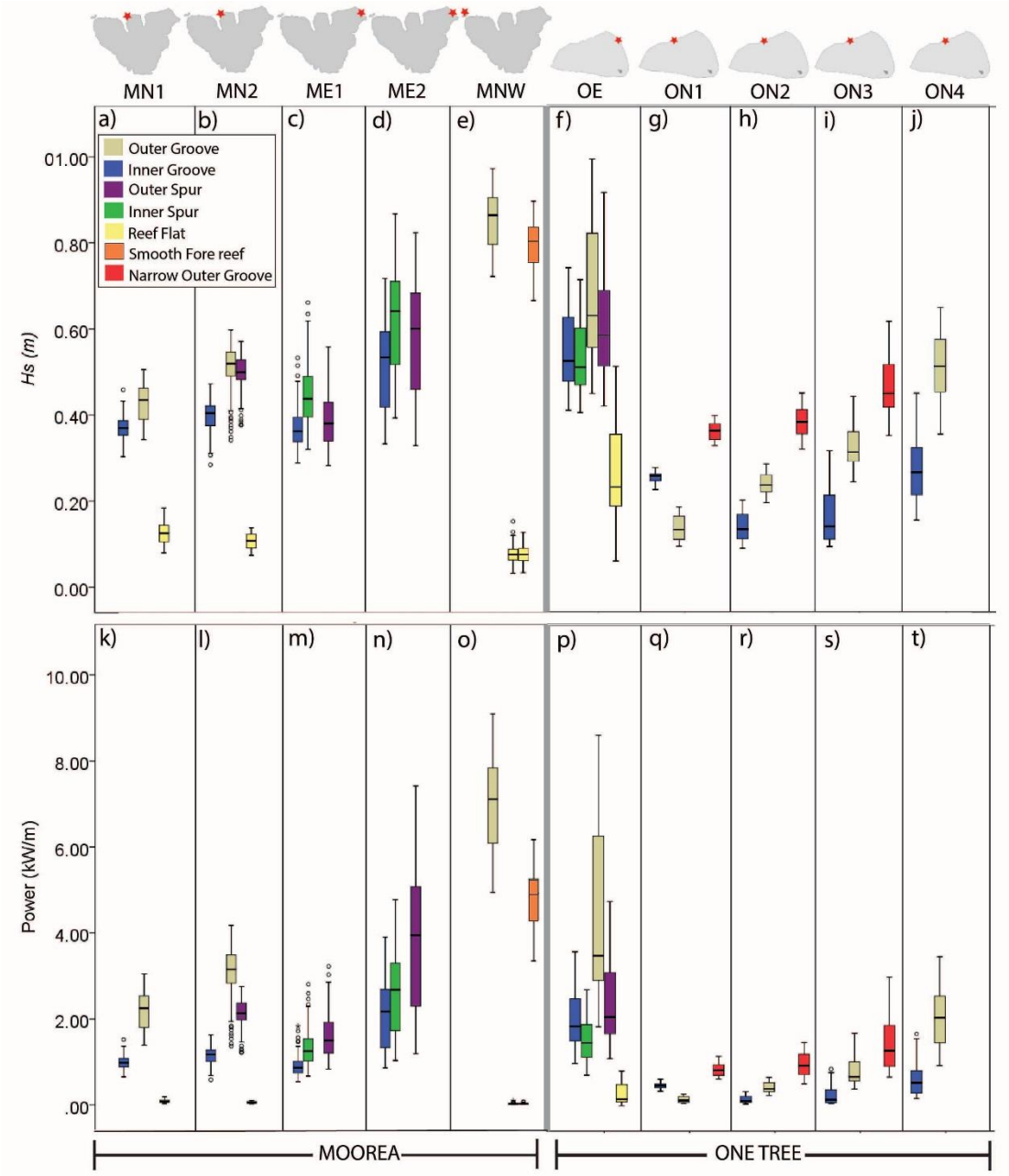


**Figure 3** Comparison of box plots showing $H_s$ (a-j) and $P$ (k-t) throughout all deployments. The colour of each box plot denotes the location of the instrument at the inner or outer groove, inner or outer spur, narrow outer groove, smooth fore reef or reef flat. Each panel is one deployment as labeled at the top. Panels a) to e) and k) to o) are Moorea deployments while f) to j) and p) to t) are One Tree deployments. Box plots show the median, first and third quartile of values recorded at each instrument during each deployment.

### 4.3 Wave energy dissipation

We found considerable variation in dissipation rates both between and within deployments. For example, the highest dissipation rate measured at One Tree East (0.1 kW/m$^2$ between the outer and inner groove) was ten times higher than the lowest dissipation rate (0.01 kW/m$^2$) between the same instruments during the same deployment (Figure 4g). The dissipation rates between the outer and inner groove were higher at the One Tree sites (OE mean $\epsilon$= 0.04 kW/m$^2$; ON = 0.06 kW/m$^2$) than the Moorea sites (MN1 mean $\epsilon$= 0.02 kW/m$^2$; MN2 = 0.03 kW/m$^2$) (Figure 4e-h). Interestingly, at both Moorea and One Tree, the rate of energy dissipation on the fore reef between the outer and inner groove was always higher than between the inner groove and the reef flat (Figure 4e-g). The greatest difference was at Moorea North during deployment 2 where the mean dissipation rate across the groove (mean $\epsilon$ =0.03 kW/m$^2$) was six times higher than across the reef crest (mean $\epsilon$ =0.005 kW/m$^2$). One Tree East was the only site where direct comparison of dissipation of across an adjacent spur and groove was possible. Somewhat surprisingly the measured dissipation rate across a groove (max = 0.1 kW/m$^2$; mean = 0.04 kW/m$^2$) was almost three times that across the adjacent spur (max = 0.048 kW/m$^2$; mean = 0.014 kW/m$^2$) (Figure 4g). This difference was most pronounced at high tide.

Most of the time the percentage of energy dissipated across the SAG zone was greater than that dissipated across the reef crest (Figure 4i-k). The maximum percentage of wave energy dissipated between the outer and inner groove was 86% at One Tree North Deployment 4 (Figure 4l) while the maximum dissipation across the reef crest was 62% at One Tree East (Figure 4k). During high tides and low wave energy conditions at Moorea North Deployment 1 and One Tree East (Figure 4i and k) the percentage dissipated across the reef crest equaled or briefly exceeded the percent dissipated across the SAG zone. During all deployments, the greatest percentage of energy dissipated by the SAG zone was during low tides with relatively high wave conditions.

The wave energy dissipation increased more sharply with *Hs* across the SAG zone than across the reef crest (Figure 5a-c). At Moorea North Deployments 1 and 2 and One Tree East percent dissipation across the SAG zone was also significantly positively correlated with *Hs* (Figure 5e-g). In contrast, percent dissipation was significantly negatively correlated with *Hs* across the reef crest. Percent dissipation and *Hs* were also negatively correlated between the wide outer and inner groove at One Tree North (Figure 5h). Across the SAG zone there is a significant negative correlation between percent dissipation and depth at all sites while across

the reef crest it is positively correlated at Moorea North but there is no relationship at One Tree East (Figure 5i-k). The positive correlation between dissipation percent and $H_s$ across the fore reef and negative correlation across the reef crest suggest bottom friction at the fore reef becomes more important for energy dissipation as wave height increases.

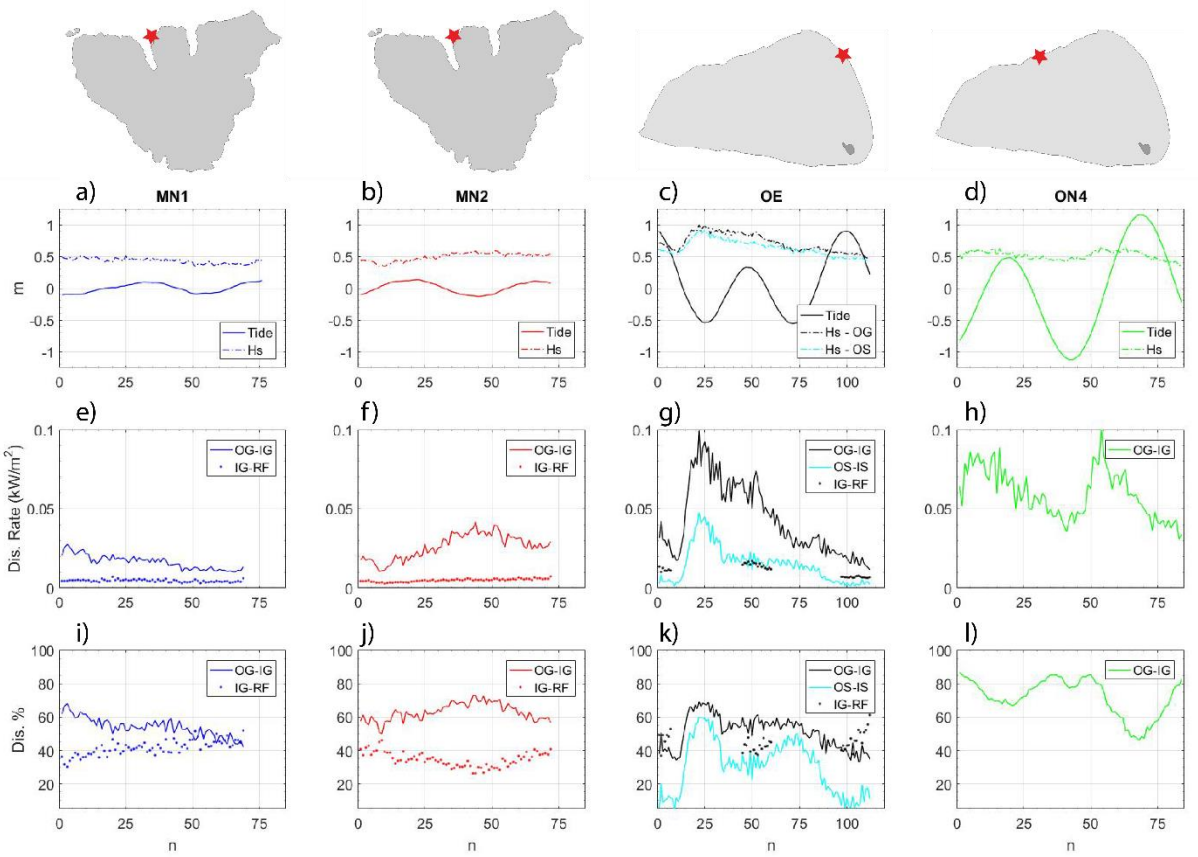


**Figure 4** Wave dissipation characteristics at Moorea North deployments 1 and 2 (MN1, MN2), One Tree East (OE) and One Tree North deployment 4 (ON4). Panels a) to d) show tidal stage and $H_s$. The rates of wave power dissipation per meter from the outer groove to the inner groove (OG – IG unbroken line) and the inner groove to the reef flat (IG – RF dotted line) are shown in panels e) to h). Note that ON4 (h) does not have IG-RF as no instrument was deployed on the reef flat. Panels i) to l) show the percentage of wave power dissipated from OG-IG (unbroken line) and IG-RF (dotted line). The x-axis is number of records, where each record accounts for 15 minutes. The reef flat at OE is sub-aerially exposed over low tidal phases therefore IG-RF calculations could only be made over high tides when waves could propagate across the reef crest. Note that deployments were not concurrent.

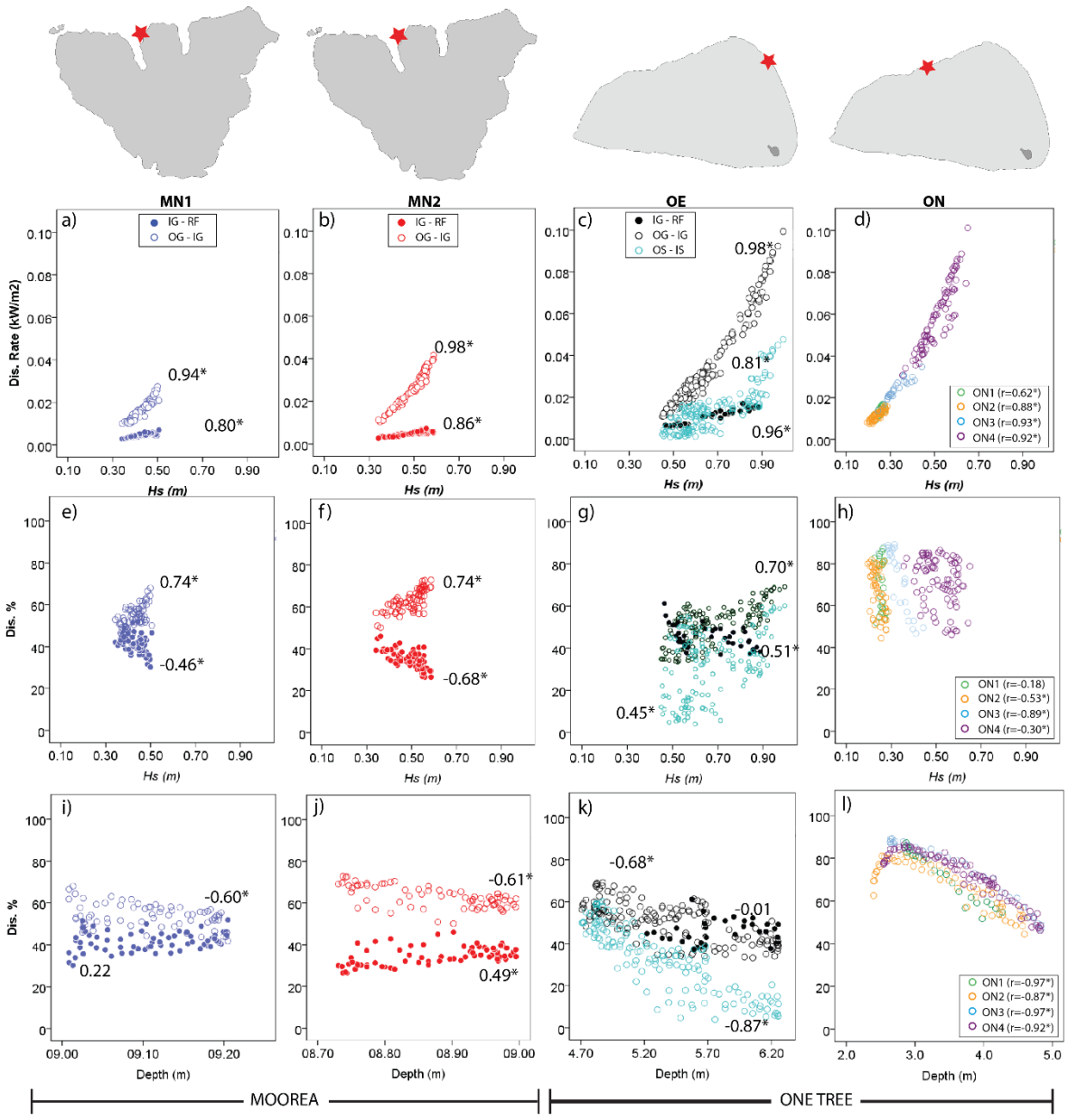


**Figure 5** Relationships between dissipation rate and *Hs* (a-d); percent of energy dissipated and *Hs* (e-h) and; percent of energy dissipated and depth (i-l) across the SAG zone from outer to inner groove (open symbols) and from inner groove to reef flat (filled symbols) at MN1, MN2, OE and ON4. Pearson's correlation r values are given with an asterisk denoting significance at the 95% level and minus signs denoting a negative correlation. Note that the x-axes of plots i-l do not have the same scale.

## 5 Discussion

### 5.1 Wave energy dissipation across the SAG zone vs the reef crest

Our study is one of the first to measure dissipation across the fore reef SAG zone and the reef crest and compare the relative importance of bottom friction and wave breaking. We found that SAG zones at Moorea and One Tree Reef dissipated between 33 to 86% of wave energy at extremely high rates (up to 0.01 - 0.1 kW/m2) through bottom friction alone (Figure 4e-g).

We found rates of wave energy dissipation across the SAG zone between the outer and inner groove, due to bottom friction, were between four and six times higher than across the reef crest where breaking likely contributed to energy dissipation (Figure 4e-h). The percentage of energy dissipated across the SAG zone was also higher than across the reef crest most of the time (Figure 4i-l). These findings call into question the long-held assumption that the vast majority of wave energy dissipation occurs at the reef crest (Ferrario et al., 2014). The importance of dissipation at the fore reef was also reported by Monismith et al. (2015) who measured rates of wave energy dissipation up to 0.03 $kW/m^2$ on the fore reef between 11.2 and 6.2 m depth at Palmyra Atoll and calculated an extremely high wave friction factor (1.80). A calibrated SWAN model for the same reef also found that the average wave dissipation rates at the fore reef due to bottom friction were larger than those due to wave breaking (Rogers et al., 2016).

We found significant positive correlations between percentage of energy dissipation and Hs across the fore reef (Figure 5e-g) and negative correlations across the reef crest. This suggests that, under the modal wave conditions measured, bottom friction at the fore reef is increasingly important for energy dissipation as wave height increases. This is somewhat consistent with modelling by Lowe et al. (2005) at Kaneohe Bay, Hawaii predicting that fore reef dissipation due to bottom friction would be greater than dissipation due to wave breaking under lower-than-average wave heights and approximately equal for average incident wave heights. For larger than average waves, their model predicted that wave breaking would become more important and dissipate energy at approximately double the rate of bottom friction. The wave heights during all our deployments were average or below average and we found rates of dissipation at the fore reef to be between 4 and 6 times the rates of dissipation across the reef crest (Figure 4e-h).

In addition to wave height, we found water depth (i.e., tidal stage) to be important in determining wave energy dissipation across the fore reef compared to the reef crest. We found that as water depth increased, the percentage of energy dissipated across the SAG zone decreased, while the percentage dissipated across the reef crest increased (Figure 5i-l). Thus, even in micro-tidal Moorea (MN1 and MN2), tidal stage played a role in the relative percentage of energy dissipated across the SAG zone as compared to the reef crest. Tidal modulation of the wave field at Moorea was also noted by Monismith et al. (2013). The decline in percent of energy dissipation with increasing water depth was particularly

pronounced at One Tree North where half as much wave energy was dissipated at high tides compared to low tides (Figure 5l). This agrees with previous findings on how propagation is controlled by tidal stage at One Tree Reef (Harris et al., 2015; Vila-Concejo et al., 2014).

The correlations we measured between percentage dissipation, Hs and water depth provide general insights into the functioning of the fore reef and reef crest and allow us to draft a conceptual model (Figure 6). Under high wave conditions and low tides the proportion of dissipation is greater at the fore reef than the reef crest because the wave base interacts with the rough and topographically complex fore reef SAGs and dissipates the majority of its energy as bottom friction before it reaches the crest. Conversely, under low wave conditions and deep water (high tides) the wave base does not reach the bed at the fore reef and more energy is dissipated at the crest. Under high wave conditions and deep water, the reef crest becomes more important, with waves breaking across the SAG as suggested by Lowe et al. (2005) and da Silva et al. (2020). At Moorea North our data showed that when $H_s$ was less than 0.5 m and water depth was approximately 0.1 m above MSL the proportions of wave energy dissipated at the fore reef and reef crest were approximately equal. While at One Tree East this occurred when water depths were ~1 m above MSL and $H_s$ was <0.75 m. Our findings that the percentage of energy dissipation at the fore reef declines with increasing depth agree with studies linking sea level rise to an increased risk of wave attack and erosion for islands and coasts currently protected by coral reefs (e.g., Albert et al. (2016), Quataert et al. (2015), Storlazzi et al. (2015) and Storlazzi et al. (2011)).

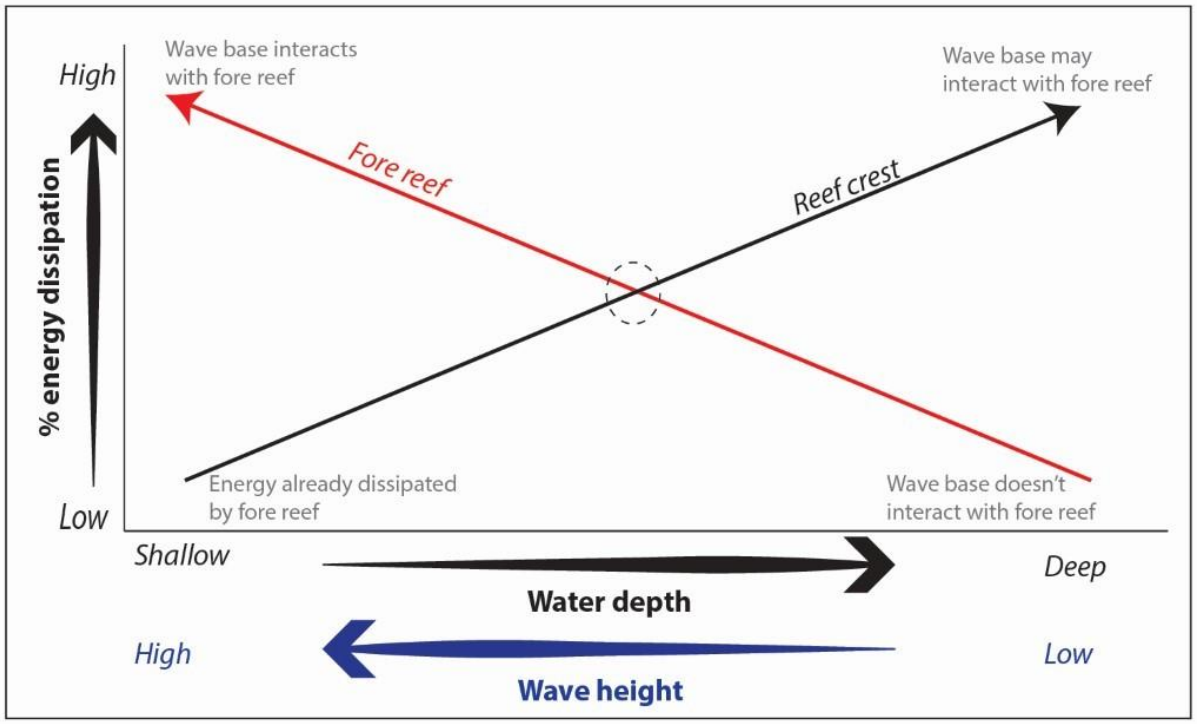


**Figure 6** Conceptual model depicting the relative percentage of wave energy dissipated at the fore reef (red line) and reef crest (black line) under different wave height and water depth conditions. Our measurements at Moorea North and One Tree East allowed us to define the water depths and wave heights at which the fore reef and reef crest will dissipate approximately equal percentages of incoming wave energy (dashed circle).

### 5.2 Global comparison of fore reef dissipation rates

An extensive literature review only found four other studies measuring wave conditions at more than one station on the fore reef allowing for calculation of fore reef wave dissipation rates (Monismith et al., 2013; Monismith et al., 2015; Pequignet et al., 2011; Storlazzi et al., 2004). The dissipation rates presented in our study are comparable to other reefs globally (Figure 7). However, one should consider that mean dissipation rate is an imperfect metric as our results demonstrate that dissipation rates are highly spatially and temporally variable and dependent on offshore wave conditions during the deployment. The highest mean dissipation rate measured across the SAG zone in this study was at One Tree North Deployment 4, on the relatively shallow, leeward side (mean $\epsilon$ = 0.056 kW/m2). Monismith et al. (2015) suggested that the relatively high dissipation rate (~0.02 kW/m2) and wave friction factor (1.8) measured at the relatively deep (11- 6 m) fore reef in Palmyra Atoll were due to high levels of live, healthy coral cover. Our study provides initial evidence to support this. Generally, we measured higher rates of dissipation across the fore reef SAG zone at One Tree (ON and OE) than at Moorea (MN1 and MN2) and the levels of live coral cover between the sites differed considerably (ON= ~85%, OE=~70%, MN=10-20%). The spurs were higher at Moorea North

than either of the One Tree sites (refer to Table 1) and the fore reef gradients at these sites were similar (ON=4°, OE=2° and MN=5°) thus it is unlikely that slope drove the difference in dissipation rates. The larger tidal range at One Tree and the associated tidal currents are also likely to play a role in wave dissipation and implies that tidal currents are likely to be an important factor modulating wave energy dissipation in meso and particularly macro tidal environments.

One Tree North may also experience offshore currents driven by wave pumping of the type reported by Callaghan et al. (2006); and Nielsen et al. (2008) whereby waves on the exposed side of the reef push water into and across the lagoon and it drains out on the leeward side. Indeed, there was greater variability in the instantaneous velocity of currents at One Tree North than at Moorea North (Duce, 2017). Further research is warranted to assess the influence of tidal currents, wave pumping, and live coral cover at the fore reef on wave energy dissipation. More data is required from multiple fore reef instrument arrays to better understand the important role of this understudied geomorphic zone in dissipating wave energy.

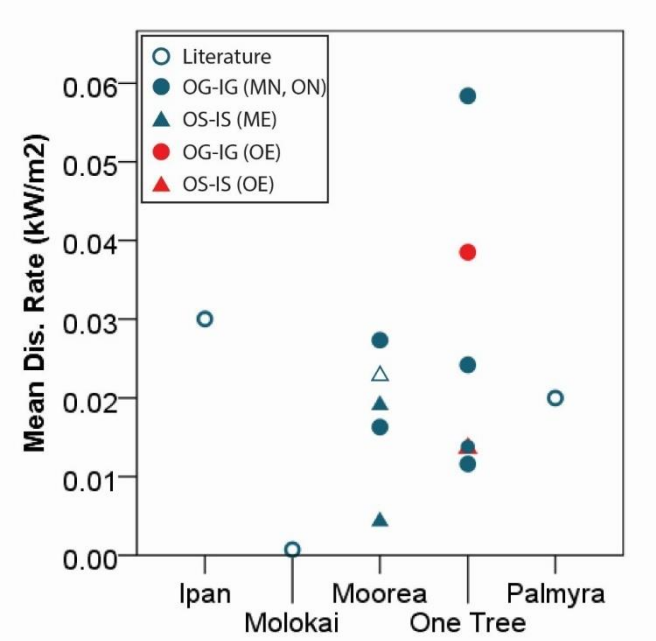


**Figure 7** Mean dissipation rates (kW/m$^2$) of wave energy across the fore reef at different sites globally. Filled symbols are deployments Moorea north (MN), One Tree north (ON), Moorea east (ME) and One Tree east (OE) with circles representing measurements between the outer and inner groove and triangles representing measurements between the outer and inner spur. Filled symbols represent measurements obtained in this study while open symbols represent values obtained from the literature. The reefs at which these rates were measured are shown on the x-axis with data derived from the following sources: Ipan, Guam (Pequignet et al., 2011); Molokai (Storlazzi et al., 2004); Moorea (this study and (Monismith et al., 2013); One Tree (this study); Palmyra Atoll (Monismith et al., 2015).

### 5.3 Comparison of wave dissipation with other ecosystems

Coral reefs provide important ecosystem services in protecting the coasts from incoming wave energy (Ferrario et al., 2014). While direct comparison is not always possible due to different methods of calculating wave dissipation, authors have shown that mangroves in Vietnam could reduce wave energy between 1.7 to 6% for every 10 m (Barbier et al., 2008). More recently, Gon et al. (2020) showed that a rock platform off Monterey Bay in California (USA) dissipated 32% over 132 m (i.e., 2.4% of the energy over 10 m). While most previous studies in reef environments presented wave dissipation over reef flats, this paper highlights the high amount of wave dissipation that occurs over the SAG on the fore reef and underlines the importance of accounting for this in future numerical modelling studies. Our results show SAG maximum (minimum) dissipation percentages over 10 m of 10.4% (6%) in Moorea and 35.9% (20.2%) at One Tree Reef. While we did not obtain detailed bathymetric data to obtain roughness or friction factors, our results demonstrate that coral reefs, and in particular SAGs, are amongst the most effective natural wave dissipaters on Earth. Temmerman et al. (2013) claimed that flood protection by ecosystem creation and restoration could provide a sustainable and cost-effective coastal engineering solution and called for implementation when possible. The coastal protection services provided by coral reefs demand global attention and conservation in light of ongoing climate change.

Numerical modelling has suggested that the structural complexity of coral reefs is more important than sea-level rise in determining the level of coastal protection provided by reefs under average wave conditions (Harris et al., 2018). An important future avenue for research includes coupling high spatial resolution (centimeter to meter scales) mapping of the 3D structure (rugosity) of reef environments (particularly the difficult to reach fore reef zone) with closely spaced instrument transects to gain an in-depth understanding of local scale turbulence and friction induced by the interaction between coral reefs with differing benthic cover and hydrodynamic forces (waves and currents).

## 6. Conclusions

We measured waves and currents in the fore reef spur and groove zone during a range of modal conditions at Moorea, French Polynesia and One Tree Reef, southern GBR, Australia. The study sites chosen had contrasting tides (micro and meso), wave regimes (exposed and sheltered), broad scale reef type (barrier reef and lagoonal platform reef), local fore reef SAG

morphology and levels of live coral cover. We found extremely high rates of wave energy dissipation (up to 0.1 kW/m$^2$) across the fore reef SAG zone due to bottom friction alone (i.e., no component of wave breaking). Under the modal conditions measured, the percent of energy dissipated at the fore reef was almost always higher than the percent dissipated across the reef crest, calling into question the dominant assumption that the reef crest is the most important geomorphic zone for energy dissipation. A conceptual model was developed showing that fore reef dissipation is more important than reef crest dissipation under high wave conditions at low tides, while reef crest dissipation is more important at high tides and small waves. In general, higher rates of dissipation were measured across SAG zones at One Tree Reef than Moorea. This may support claims that higher live coral cover produces greater bottom friction and wave dissipation though more research is required. It also suggests the importance of tidal currents in influencing wave energy dissipation. Longer deployments, capturing a range of hydrodynamic driving conditions, with instruments at inner and outer ends of both spurs and grooves are required to better understand the complex nature of morphodynamic feedbacks in this important zone.

**Acknowledgements**

We gratefully acknowledge funding from a Tempe Mann Travelling Scholarship from the Australian Federation of Graduate Women (S.D.), an Australian Postgraduate Award (S.D.), a University of Sydney Merit Award (S.D), a Great Barrier Reef Marine Park Authority Science for Management Award (S.D. 9/1667(2)) an ARC Future Fellowship (A.V.C., FT100100215) and return to work grant for Women in Science at the University of Sydney (AVC). We also thank staff at CRIOBE research station and One Tree Island Research Station. The help of field volunteers Russell Graham, Glen Shaw, Matt Kosnik, Andrew Irving, Pepe Brennen, Vetea Liao, Andrew Durrant, Selma Klanten, Jonathan Walsh and Aero Leplastrier is greatly appreciated. Offshore wave data sets were provided by the Moorea Coral Reef Ecosystem Long-Term Ecological Research (LTER) program, funded by the US National Science Foundation (OCE-0417412) and the Queensland Integrated Marine Observing System (Q-IMOS) operated by the Australian Institute of Marine Science with the assistance of Craig Steinberg. Datasets for this research are available from Figshare: https://figshare.com/articles/dataset/SAG_Hydrodynamics_Datasets_Moorea_and_One_Tree/14036747.

**References**

Adjeroud, M., Michonneau, F., Edmunds, P. J., Chancerelle, Y., de Loma, T. L., Penin, L., . . . Galzin, R. (2009). Recurrent disturbances, recovery trajectories, and resilience of coral assemblages on a South Central Pacific reef. *Coral Reefs, 28*(3), 775-780. doi:10.1007/s00338-009-0515-7

Albert, S., Leon, J. X., Grinham, A. R., Church, J. A., Gibbes, B. R., & Woodroffe, C. D. (2016). Interactions between sea-level rise and wave exposure on reef island dynamics in the Solomon Islands. *Environmental Research Letters, 11*(5), 1-9.

Baldock, T. E., Shabani, B., & Callaghan, D. P. (2019). Open access Bayesian Belief Networks for estimating the hydrodynamics and shoreline response behind fringing reefs subject to climate changes and reef degradation. *Environmental Modelling and Software, 119*(June), 327-340. doi:10.1016/j.envsoft.2019.07.001

Baldock, T. E., Shabani, B., Callaghan, D. P., Hu, Z., & Mumby, P. J. (2020). Two-dimensional modelling of wave dynamics and wave forces on fringing coral reefs. *Coastal Engineering, 155*. doi:10.1016/j.coastaleng.2019.103594

Barbier, E. B., Koch, E. W., Silliman, B. R., Hacker, S. D., Wolanski, E., Primavera, J., . . . Reed, D. J. (2008). Coastal ecosystem-based management with nonlinear ecological functions and values. *Science, 319*(5861), 321-323. doi:10.1126/science.1150349

Beck, M. W., Losada, I. J., Menéndez, P., Reguero, B. G., Díaz-Simal, P., & Fernández, F. (2018). The global flood protection savings provided by coral reefs. *Nature Communications, 9*(1). doi:10.1038/s41467-018-04568-z

Beetham, E. P., & Kench, P. S. (2014). Wave energy gradients and shoreline change on Vabbinfaru platform, Maldives. *Geomorphology, 209*, 98-110. doi:10.1016/j.geomorph.2013.11.029

Bramante, J. F., Ashton, A. D., Storlazzi, C. D., Cheriton, O. M., & Donnelly, J. P. (2020). Sea-level rise will drive divergent sediment transport patterns on fore reefs and reef flats, potentially causing erosion on atoll islands. *Journal of Geophysical Research: Earth Surface*. doi:10.1029/2019jf005446

Brander, R. W., Kench, P. S., & Hart, D. (2004). Spatial and temporal variations in wave characteristics across a reef platform, Warraber Island, Torres Strait, Australia. *Marine Geology, 207*(1-4), 169-184. doi:10.1016/j.margeo.2004.03.014

Bryson, M., Duce, S., Harris, D., Webster, J. M., Thompson, A., Vila-Concejo, A., & Williams, S. B. (2016). Geomorphic changes of a coral shingle cay measured using Kite Aerial Photography. *Geomorphology, 270*, 1-8. doi:10.1016/j.geomorph.2016.06.018

Callaghan, D. P., Nielsen, P., Cartwright, N., Gourlay, M. R., & Baldock, T. E. (2006). Atoll lagoon flushing forced by waves. *Coastal Engineering, 53*(8), 691-704. doi:http://dx.doi.org/10.1016/j.coastaleng.2006.02.006

Cheriton, O. M., C. D. Storlazzi and K. J. Rosenberger (2016). "Observations of wave transformation over a fringing coral reef and the importance of low-frequency waves and offshore water levels to runup, overwash and coastal flooding." *Journal of Geophysical Research: Oceans* 121.

da Silva, R. F., Storlazzi, C. D., Rogers, J. S., Reyns, J., & McCall, R. (2020). Modelling three-dimensional flow over spur-and-groove morphology. *Coral Reefs*. doi:10.1007/s00338-020-02011-8

Duce, S. (2017). *The Form, Function and Evolution of Coral Reef Spur and Grooves.* (Unpublished PhD Thesis). University of Sydney, Sydney, Australia.

Duce, S., Dechnik, B., Webster, J. M., Hua, Q., Sadler, J., Webb, G. E., . . . Vila-Concejo, A. (2020). Mechanisms of spur and groove development and implications for reef platform evolution. *Quaternary Science Reviews, 231*, 106155. doi:https://doi.org/10.1016/j.quascirev.2019.106155

Duce, S., Vila-Concejo, A., Hamylton, S. M., Webster, J. M., Bruce, E., & Beaman, R. J. (2016). A morphometric assessment and classification of coral reef spur and groove morphology. *Geomorphology, 265*, 68-83.

Edmunds, P. J., & Leichter, J. J. (2016). Spatial scale-dependent vertical zonation of coral reef community structure in French Polynesia. *Ecosphere, 7*(5), 1-14. doi:10.1002/ecs2.1342

Etienne, S. (2012). Marine inundation hazards in French Polynesia: Geomorphic impacts of tropical cyclone oli in February 2010. *Geological Society Special Publication, 361*(1), 21-39. doi:10.1144/SP361.4

Ferrario, F., Beck, M. W., Storlazzi, C. D., Micheli, F., Shepard, C. C., & Airoldi, L. (2014). The effectiveness of coral reefs for coastal hazard risk reduction and adaptation. *Nature Communications, 5*, 3794. doi:10.1038/ncomms4794

Foley, M., Stender, Y., Singh, A., Jokiel, P., & Rodgers, K. u. (2014). Ecological Engineering Considerations for Coral Reefs in the Design of Multifunctional Coastal Structures. *Coastal Engineering Proceedings, 1*(34), 30-30. doi:10.9753/icce.v34.management.30

Frith, C. A., & Mason, L. B. (1986). Modelling wind driven circulation One Tree Reef, Southern Great Barrier Reef. *Coral Reefs, 4*(4), 201-211. doi:10.1007/BF00298078

Gallop, S. L., Young, I. R., Ranasinghe, R., Durrant, T. H., & Haigh, I. D. (2014). The large-scale influence of the Great Barrier Reef matrix on wave attenuation. *Coral Reefs, 33*(4), 1167-1178. doi:10.1007/s00338-014-1205-7

Gischler, E. (2010). Indo-Pacific and Atlantic spurs and grooves revisited: The possible effects of different Holocene sea-level history, exposure, and reef accretion rate in the shallow fore reef. *Facies, 56*(2), 173-177. doi:10.1007/s10347-010-0218-0

Gon, C. J., MacMahan, J. H., Thornton, E. B., & Denny, M. (2020). Wave Dissipation by Bottom Friction on the Inner Shelf of a Rocky Shore. *Journal of Geophysical Research: Oceans, 125*(10). doi:10.1029/2019jc015963

Hamylton, S., Silverman, J., & Shaw, E. (2013). The use of remote sensing to scale up measures of carbonate production on reef systems: a comparison of hydrochemical and census-based estimation methods. *International Journal of Remote Sensing, 34*(18), 6451-6465. doi:10.1080/01431161.2013.800654

Hardy, T. A., & Young, I. R. (1996). Field study of wave attenuation on an offshore coral reef. *Journal of Geophysical Research: Oceans, 101*(C6), 14311-14326. doi:10.1029/96JC00202

Harris, D. L., Rovere, A., Casella, E., Power, H. E., Canavesio, R., Collin, A., . . . Parravicini, V. (2018). Coral reef structural complexity provides important coastal protection from waves under rising sea levels. *Science Advances, 4*(2), 1-7. doi:10.1126/sciadv.aao4350

Harris, D. L., & Vila-Concejo, A. (2013). Wave transformation on a coral reef rubble platform. *Journal of Coastal Research, 65*, 506-510. doi:10.2112/si65-086.1

Harris, D. L., Vila-Concejo, A., Webster, J. M., & Power, H. E. (2015). Spatial variations in wave transformation and sediment entrainment on a coral reef sand apron. *Marine Geology, 363*, 220-229. doi:10.1016/j.margeo.2015.02.010

Hench, J. L., Leichter, J. J., & Monismith, S. G. (2008). Episodic circulation and exchange in a wave-driven coral reef and lagoon system. *Limnology and Oceanography, 53*(6), 2681-2694. doi:10.4319/lo.2008.53.6.2681

Hopley, D., Smithers, S. G., & Parnell, K. E. (2007). *The Geomorphology of the Great Barrier Reef : development, diversity, and change*. Cambridge: Cambridge University Press.

Horstman, E. M., Dohmen-Janssen, C. M., Narra, P. M. F., van den Berg, N. J. F., Siemerink, M., & Hulscher, S. J. M. H. (2014). Wave attenuation in mangroves: A quantitative approach to field observations. *Coastal Engineering, 94*, 47-62. doi:10.1016/j.coastaleng.2014.08.005

Huang, Z. C., Lenain, L., Melville, W. K., Middleton, J. H., Reineman, B., Statom, N., & McCabe, R. M. (2012). Dissipation of wave energy and turbulence in a shallow coral reef lagoon. *Journal of Geophysical Research: Oceans, 117*(3), 1-18. doi:10.1029/2011JC007202

Kayal, M., Vercelloni, J., Lison de Loma, T., Bosserelle, P., Chancerelle, Y., Geoffroy, S., . . . Adjeroud, M. (2012). Predator Crown-of-Thorns Starfish (Acanthaster planci) Outbreak, Mass Mortality of Corals, and Cascading Effects on Reef Fish and Benthic Communities. *PLoS ONE, 7*(10). doi:10.1371/journal.pone.0047363

641 Kench, P. S., & Brander, R. W. (2006). Wave Processes on Coral Reef Flats: Implications for Reef
642 Geomorphology Using Australian Case Studies. *Journal of Coastal Research, 221*, 209-223.
643 doi:10.2112/05a-0016.1
644 Kench, P. S., Brander, R. W., Parnell, K. E., & O'Callaghan, J. M. (2009). Seasonal variations in wave
645 characteristics around a coral reef island, South Maalhosmadulu atoll, Maldives. *Marine*
646 *Geology, 262*(1-4), 116-129. doi:10.1016/j.margeo.2009.03.018
647 Lee, D.-Y., & Wang, H. (1984). Measurement of surface waves from subsurface gage. *Coastal*
648 *Engineering Proceedings, 1*(19), 271-286.
649 Leichter, J. J., Alldredge, A. L., Bernardi, G., Brooks, A. J., Carlson, C. A., Carpenter, R. C., . . . Wyatt, A.
650 S. J. (2013). Biological and Physical Interactions on a Tropical Island Coral Reef: Transport
651 and Retention Processes on Morea, French Polynesia. *Oceanographic Society, 26*(3), 52-63.
652 Leichter, J. J., Stokes, M. D., Hench, J. L., Witting, J., & Washburn, L. (2012). The island-scale internal
653 wave climate of Moorea, French Polynesia. *Journal of Geophysical Research: Oceans, 117*(6),
654 1-16. doi:10.1029/2012JC007949
655 Lowe, R. J. (2005). Spectral wave dissipation over a barrier reef. *Journal of Geophysical Research,*
656 *110*(C4), C04001-C04001. doi:10.1029/2004JC002711
657 Lowe, R. J., Falter, J. L., Bandet, M. D., Pawlak, G., Atkinson, M. J., Monismith, S. G., & Koseff, J. R.
658 (2005). Spectral wave dissipation over a barrier reef. *J. Geophys. Res, 110*, 4001-4001.
659 doi:10.1029/2004JC002711
660 Lugo-Fernández, A., Roberts, H. H., & Suhayda, J. N. (1998a). Wave transformations across a
661 caribbean fringing-barrier Coral Reef. *Continental Shelf Research, 18*(10), 1099-1124.
662 doi:10.1016/S0278-4343(97)00020-4
663 Lugo-Fernández, A., Roberts, H. H., & Wiseman, W. J. (1998b). Tide effects on wave attenuation and
664 wave set-up on a Caribbean coral reef. *Estuarine, Coastal and Shelf Science, 47*(4), 385-393.
665 doi:10.1006/ecss.1998.0365
666 Mandlier, P. G. (2013). Field observations of wave refraction and propagation pathways on coral reef
667 platforms. *Earth Surface Processes and Landforms, 38*(9), 913-925. doi:10.1002/esp.3328
668 Masselink, G., Beetham, E., & Kench, P. (2020). Coral reef islands can accrete vertically in response to
669 sea level rise. *Sci. Adv, 6*(June), 3656-3666. Retrieved from http://advances.sciencemag.org/
670 Monismith, S. G., Herdman, L. M. M., Ahmerkamp, S., & Hench, J. L. (2013). Wave Transformation
671 and Wave-Driven Flow across a Steep Coral Reef. *Journal of Physical Oceanography, 43*(7),
672 1356-1379. doi:10.1175/jpo-d-12-0164.1
673 Monismith, S. G., Rogers, J. S., Koweek, D., & Dunbar, R. B. (2015). Frictional wave dissipation on a
674 remarkably rough reef. *Geophysical Research Letters, 42*(10), 4063-4071.
675 doi:10.1002/2015GL063804
676 Munk, W. H., & Sargent, M. C. (1948). Adjustment of Bikini Atoll to ocean waves. *Transactions,*
677 *American Geophysical Union, 29*(6), 855-855. doi:10.1029/TR029i006p00855
678 Nielsen, P., Guard, P. A., Callaghan, D. P., & Baldock, T. E. (2008). Observations of wave pump
679 efficiency. *Coastal Engineering, 55*(1), 69-72.
680 doi:http://dx.doi.org/10.1016/j.coastaleng.2007.07.003
681 Pequignet, A.-C., Becker, J. M., Merrifield, M. A., & Boc, S. J. (2011). The dissipation of wind wave
682 energy across a fringing reef at Ipan, Guam. *Coral Reefs, 30*, 71-82.
683 Péquignet, A. C., Becker, J. M., Merrifield, M. A., & Boc, S. J. (2011). The dissipation of wind wave
684 energy across a fringing reef at Ipan, Guam. *Coral Reefs, 30*(SUPPL. 1), 71-82.
685 doi:10.1007/s00338-011-0719-5
686 Pomeroy, A., Lowe, R., Symonds, G., Van Dongeren, A., & Moore, C. (2012). The dynamics of
687 infragravity wave transformation over a fringing reef. *Journal of Geophysical Research:*
688 *Oceans, 117*(11). doi:10.1029/2012JC008310
689 Quataert, E., Storlazzi, C., van Rooijen, A., Cheriton, O., & van Dongeren, A. (2015). The influence of
690 coral reefs and climate change on wave-driven flooding of tropical coastlines. *Geophysical*
691 *Research Letters, 42*(15), 6407-6415. doi:10.1002/2015GL064861

692 Roberts, H. H. (1974). *Variability of reefs with regard to changes in wave power around an island.*
693 Paper presented at the Proceedings of the Second International Symposium on Coral Reefs,
694 Brisbane, Brisbane, Australia.
695 Roberts, H. H., Murray, S. P., & Suhayda, J. N. (1975). Physical Processes in Fringing Reef System.
696 *Journal of Marine Research, 33*(2), 233-260. Retrieved from <Go to
697 ISI>://WOS:A1975AL34800006
698 Rogers, J. S., Monismith, S. G., Koweek, D., & Dunbar, R. B. (2016). Wave Dynamics of a Pacific Atoll
699 with High Friction. *Journal of Geophysical Research - Oceans, 120*, 1-18.
700 Samosorn, B., & Woodroffe, C. D. (2008). Nearshore wave environments around a sandy cay on a
701 platform reef, Torres Strait, Australia. *Continental Shelf Research, 28*(16), 2257-2274.
702 doi:10.1016/j.csr.2008.03.043
703 Shannon, A. M., Power, H. E., Webster, J. M., & Vila-Concejo, A. (2013). Evolution of coral rubble
704 deposits on a reef platform as detected by remote sensing. *Remote Sensing, 5*(1), 1-18.
705 doi:10.3390/rs5010001
706 Storlazzi, C. D., Brown, E. K., Field, M. E., Rodgers, K., & Jokiel, P. L. (2005). A model for wave control
707 on coral breakage and species distribution in the Hawaiian Islands. *Coral Reefs, 24*(1), 43-55.
708 doi:10.1007/s00338-004-0430-x
709 Storlazzi, C. D., Elias, E., Field, M. E., & Presto, M. K. (2011). Numerical modeling of the impact of sea-
710 level rise on fringing coral reef hydrodynamics and sediment transport. *Coral Reefs,*
711 *30*(SUPPL. 1), 83-96. doi:10.1007/s00338-011-0723-9
712 Storlazzi, C. D., Elias, E. P. L., & Berkowitz, P. (2015). Many Atolls May be Uninhabitable Within
713 Decades Due to Climate Change. *Scientific Reports, 5*(1), 1-9. doi:10.1038/srep14546
714 Storlazzi, C. D., Logan, J. B., & Field, M. E. (2003). Quantitative morphology of a fringing reef tract
715 from high-resolution laser bathymetry: Southern Molokai, Hawaii. *Geological Society of*
716 *America Bulletin, 115*(11), 1344-1355. doi:10.1130/b25200.1
717 Storlazzi, C. D., Ogston, A. S., Bothner, M. H., Field, M. E., & Presto, M. K. (2004). Wave-and tidally-
718 driven flow and sediment flux across a fringing coral reef: Southern Molokai, Hawaii.
719 *Continental Shelf Research, 24*, 1397-1419. doi:10.1016/j.csr.2004.02.010
720 Temmerman, S., Meire, P., Bouma, T. J., Herman, P. M. J., Ysebaert, T., & De Vriend, H. J. (2013).
721 Ecosystem-based coastal defence in the face of global change. In (Vol. 504, pp. 79-83).
722 Tolman, H. L. (2009). *User manual and system documentation of WAVEWATCH III version 3.14*.
723 Retrieved from https://polar.ncep.noaa.gov/mmab/papers/tn276/MMAB_276.pdf
724 Trapon, M. L., Pratchett, M. S., & Penin, L. (2011). Comparative Effects of Different Disturbances in
725 Coral Reef Habitats in Moorea, French Polynesia. *Journal of Marine Biology, 2011*, 1-11.
726 doi:10.1155/2011/807625
727 Van Zanten, B. T., Van Beukering, P. J. H., & Wagtendonk, A. J. (2014). Coastal protection by coral
728 reefs: A framework for spatial assessment and economic valuation. *Ocean and Coastal*
729 *Management, 96*, 94-103. doi:10.1016/j.ocecoaman.2014.05.001
730 Vetter, O., Becker, J. M., Merrifield, M. A., Pequignet, A. C., Aucan, J., Boc, S. J., & Pollock, C. E.
731 (2010). Wave setup over a Pacific Island fringing reef. *Journal of Geophysical Research-*
732 *Oceans, 115*, 1-13. doi:10.1029/2010jc006455
733 Vila-Concejo, A., Duce, S., Nagao, M., Nakashima, Y., Ito, M., Fujita, K., & Kan, H. (2017). Typhoon
734 Waves on Coral Reefs. *Coastal Dynamics 2017*(263), 697-701.
735 Vila-Concejo, A., Harris, D. L., Power, H. E., Shannon, A. M., & Webster, J. M. (2014). Sediment
736 transport and mixing depth on a coral reef sand apron. *Geomorphology, 222*, 143-150.
737 doi:10.1016/j.geomorph.2013.09.034
738 Washburn, L. (2015). *MCR LTER: Coral Reef Ocean Currents and Biogeochemistry: salinity,*
739 *temperature and current at CTD and ADCP mooring FOR01 from 2004 ongoing*.
740 Washburn, L., & Brooks, A. J. (2016). *MCR LTER: Coral Reef: Gump Station Meterorological Data,*
741 *ongoing since 2006. knb-lter-mcr.9.41*

Woodhead, A. J., Hicks, C. C., Norström, A. V., Williams, G. J., & Graham, N. A. J. (2019). Coral reef ecosystem services in the Anthropocene. *Functional Ecology, 33*(6), 1023-1034. doi:10.1111/1365-2435.13331

Woolsey, E., Bainbridge, S. J., Kingsford, M. J., & Byrne, M. (2012). Impacts of cyclone Hamish at One Tree Reef: Integrating environmental and benthic habitat data. *Marine Biology, 159*(4), 793-803. doi:10.1007/s00227-011-1855-8